*Journal of Neurocytology* **21**, 185–197 (1992)

# BUdR as an S-phase marker for quantitative studies of cytokinetic behaviour in the murine cerebral ventricular zone

T. TAKAHASHI[1]*, R. S. NOWAKOWSKI[2], and V. S. CAVINESS, JR[1]

[1] *Department of Neurology, Massachusetts General Hospital, Harvard Medical School, Boston, MA, 02114, USA*
[2] *Department of Neuroscience and Cell Biology, UMDNJ-Robert Wood Johnson Medical School, Piscataway, NJ 08854, USA*

Received 30 August 1991; revised 30 October 1991; accepted 1 November 1991

## Summary

BUdR incorporation into replicating DNA, detected immunohistochemically, is used as an S-phase marker in the proliferative cell populations of the cerebral wall of the mouse embryo on the 14th gestational day (E14). The analysis initiates a series of studies concerned with the cytokinetic behaviour and cell output of proliferative populations involved in neocortical histogenesis. On E14 there are two periventricular proliferative zones in the cerebral wall. These are the ventricular and subventricular zones. The ventricular zone is a pseudostratified epithelium. DNA replication occurs with the cell nucleus in the outer zone of the epithelium and mitoses at the ventricular surface. Prior applications of BUdR for studies of cytogenesis in the CNS have been extended in two principal ways: (1) basic fuchsin was used as counterstain for BUdR-negative nuclei and (2) labelling indices were determined separately in strata or bins, 10 μm in height, through the full depth of the ventricular zone and overlying cerebral wall.

It was established that a single injection of 50 $\mu g\ g^{-1}$ into the pregnant dam was associated with labelling of 100% of nuclei in S-phase over an interval extending from 15 min to at least 2.0 h after injection. The zone where nuclei are undergoing S-phase (S-phase zone) extends through the outer four bins of the ventricular zone. The method has high quantitative reproducibility with an SE for labelling indices in bins within the S-phase zone less than 10% of the average values. Evidence is provided that BUdR incorporation is initiated with the nucleus in the outer aspect of the S-phase zone. The efficiency of incorporation of the marker is reduced as nuclei near the end of DNA replication and move to the inner aspect of the S-phase zone.

## Introduction

Neural cell proliferation in much of the developing CNS occurs in two specialized zones, the ventricular zone (VZ) and the subventricular zone (SVZ), which line the ventricular cavities of the developing brain and spinal cord (Boulder Committee, 1970). Neurons destined for most CNS structures undergo their divisions within these proliferative zones and then migrate to their definitive positions (Angevine & Sidman, 1961; Berry *et al.*, 1964; Rakic, 1972, 1978, 1988; Caviness & Sidman, 1973; Shoukimas & Hinds, 1978; Nowakowski & Rakic, 1981; Caviness, 1982; Misson *et al.*, 1991). Glial cells, by contrast, may remain in the proliferative zone after exiting the cell cycle or may retain their proliferative potential after exiting these primary proliferative zones (Smart, 1961; Smart & Leblond, 1961; Altman, 1966; Mares & Bruckner, 1978; Schmechel & Rakic, 1979; Rakic, 1985; Takamiya *et al.*, 1988).

The relative position of the nucleus of a proliferative cell in the VZ relates to its position in the cell cycle (His, 1904; Sauer, 1935; Sauer & Walker, 1959; Sidman *et al.*, 1959; Fujita, 1960, 1963; Hinds & Ruffett, 1971). Thus, nuclei in mitosis (M-phase) are located at the ventricular surface; those in the DNA synthetic phase (S-phase) are located at the outer or abventricular aspect of the VZ (S-phase zone), and those in interphases (G1- and G2-phases) are at intermediate depths (Fig. 1). The extent of the SVZ is not defined architectonically. It is adjacent to the VZ and contains proliferating cells which undergo their mitotic divisions at some distance from the ventricular surface.

The duration of each of the phases of the cell cycle in

* To whom correspondence should be addressed

0300–4864/92 $03.00 +.12 

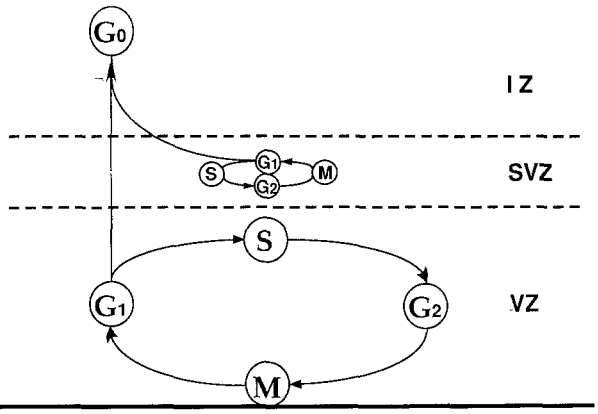


**Fig. 1.** Schematic representation of interkinetic movement of nuclei within the generative epithelium. Cell proliferation in the developing neocortex occurs in two specialized zones, the ventricular zone (VZ) and the subventricular zone (SVZ). The relative position of the cell nucleus in the VZ is related to its position in the proliferative cycle. Nuclei in the DNA synthetic phase are located at the outer, or abventricular, aspect of the VZ (S); those in M-phase are at the ventricular surface (M) and those in interphases are at intermediate depths (G1 and G2). In the SVZ proliferating cells undergo their mitotic divisions without moving away from or towards the ventricular surface. Postmitotic cells (GO) leave the cell cycle and migrate from the proliferative zones across the intermediate zone (IZ) to reach their final destinations.

rodents has been estimated by methods based upon autoradiography, where S-phase cells are marked by tritiated thymidine ($^3$H-TdR) (Fujita *et al.*, 1964, 1966; Atlas & Bond, 1965; Kauffman, 1966, 1968; Shimada & Langman, 1970; Sidman, 1970; Waechter & Jaensch, 1972). More recently the length of the cell cycle and of the S-phase were measured using immunohistochemical methods to detect 5-bromo-2'-deoxyuridine (BUdR) incorporated into DNA (Gratzner, 1982; Miller & Nowakowski, 1988, 1991; Nowakowski *et al.*, 1989).

The present analysis is the first in a series of experiments in mice, based upon S-phase marking with BUdR, which will study the cytokinetics and cell cycle output occurring in the course of histogenesis of the neocortex. BUdR offers the substantial advantages over $^3$H-TdR that the marker can be recognized within the tissue plane itself and that there is essentially no 'background' staining. The analysis is undertaken in the dorsomedial region of the cerebral wall at embryonic day 14 (E14). This gestational day is a critical time in neocortical histogenesis, corresponding to the stage when there is an apparent dramatic surge in neurogenesis concurrent with the establishment of the complete pattern of architectonic stratification of the cerebral wall. This initial stage of the analysis (1) establishes quantitative bounds of reproducibility of the BUdR labelling method, (2) develops a quantitative BUdR-based method for characterizing cytokinetic behaviour within the VZ and (3) characterizes the initial patterns of interkinetic movement of nuclei containing BUdR-labelled chromatin.

## Materials and methods

### *Animals*

CD1 mice, used for these studies, were maintained on a 12 h (7am–7pm) light–dark schedule. Conception was ascertained by the presence of a vaginal plug with the day of conception considered to be E0. Plug checks were conducted at 9:00 am.

### *BUdR injection schedules*

Pregnant mice were injected intraperitoneally with BUdR (Sigma; 5 mg ml$^{-1}$ in saline solution which was 0.007 N for sodium hydroxide). Single injections or the initial injection of a cumulative labelling sequence (Nowakowski *et al.*, 1989) were given at 9:00 am on E14 (Table 1). Individual injections were given at a maximum dose of 50 μg g$^{-1}$ body weight and also at 25 μg g$^{-1}$ (one-half the maximum dose of 50 μg g$^{-1}$) and 6.25 μg g$^{-1}$ (one-eighth the maximum dose of 50 μg g$^{-1}$). The maximum dose employed here was that used previously to label 100% of nuclei in S-phase ('saturation' labelling of S-phase nuclei) without apparent cytotoxicity (Miller & Nowakowski, 1988; Nowakowski *et al.*, 1989).

The injections were given according to four schedules where both interinjection intervals and BUdR doses were varied (Table 1). In an initial set of studies with serial injections, two injections of 50 μg g$^{-1}$ were given with either 1.5 or 3.0 h interinjection intervals. These intervals were adopted because they had been found to be shorter than the length of S-phase in previous experiments in rodents (Fujita *et al.*, 1964; Kauffman, 1966, 1968; Atlas & Bond, 1965; Shimada & Langman, 1970; Waechter & Jaensch, 1972; Miller & Nowakowski, 1991). These interinjection intervals were expected to assure saturation labelling of S-phase nuclei.

For the second set of studies, 50 μg g$^{-1}$ BUdR was given as a single injection with survival times ranging from 10 min to 3.5 h. These studies were to establish the minimal and maximal survival times after injection during which this dose of BUdR would provide saturation labelling of S-phase nuclei. Finally, in the third and fourth set of experiments, there were explorations of the labelling effectiveness of doses less than 50 μg g$^{-1}$ (25 and 6.25 μg g$^{-1}$).

Following the practice of Nowakowski and colleagues (1989), a period of 30 min between the last BUdR injection and killing was adopted for cumulative labelling experiments. It was confirmed in the present experiments that this interval is sufficient because it is greater than the minimal time required for saturation labelling of S-phase nuclei after a single BUdR injection at a dose of 50 μg g$^{-1}$

### *Immunohistochemistry*

Embryos were removed by hysterotomy from dams deeply anaesthetized with a mixture of Ketamine (50 mg kg$^{-1}$ body weight) and Xylazine (10 mg kg$^{-1}$ body weight). The embryos were decapitated, and the whole heads were fixed overnight by immersion in 70% ethanol, then dehydrated in

**Table 1.** BUdR injection schedules

| *Time* | 9:00 am | | | | | | 10:00 | | 11:00 | | 12:00 | |
|---|---|---|---|---|---|---|---|---|---|---|---|---|
| *Elapsed time* | 0:00 | 0:10 | 0:15 | 0:20 | 0:25 | 0:30 | 1:00 | 1:30 | 2:00 | 2:30 | 3:00 | 3:30 |
| (1) Cumulative injection; 50 μg $g^{-1}$ (maximum) | I | | | | | | | I | K | | | |
| | I | | | | | | | | | | I | K |
| (2) Single injection; 50 μg $g^{-1}$ (maximum) | I | K | | | | | | | | | | |
| | I | | K | | | | | | | | | |
| | I | | | K | | | | | | | | |
| | I | | | | K | | | | | | | |
| | I | | | | | K | | | | | | |
| | I | | | | | | | | K | | | |
| | I | | | | | | | | | | | K |
| (3) Single injection; 25 μg $g^{-1}$ (maximum/2) | I | | | | | K | | | | | | |
| | I | | | | | | | | K | | | |
| (4) Single injection; 6.25 μg $g^{-1}$ (maximum/8) | I | | | | | K | | | | | | |

A total of six animals from two litters (at least two animals from each litter) were analyzed for each of these schedules. I: injection K: killed

graded ethanol solutions and xylene. The brains were then immersed overnight in paraffin at 58° C, embedded in paraffin and sectioned at 4 μm in the coronal plane. The sections were mounted on glass slides that had been previously coated with a mixture of equal amounts of glycerol and 10% albumin.

The sections were deparaffinized with xylene, rehydrated in graded ethanol solutions and rinsed with 0.05 M phosphate buffered saline (PBS, pH 7.4). Following 1 h in 2 N HCl at room temperature to hydrolyze partially the double stranded DNA into single strands, the sections were rinsed with 0.1 M PBS (pH 6.0) for 30 s and incubated with anti-BUdR antibody (diluted 1:75 in PBS, pH 7.4; Becton-Dickenson) containing a detergent (0.5% Tween-20) at room temperature for 30 min. The sections were rinsed with 0.45% biotinylated anti-mouse IgG in PBS (pH 7.4) with 1.5% normal horse serum for 45 min at room temperature and then with 1.8% avidin-bound peroxidase complex (ABC Elite kit, Vector) in PBS (pH 7.4) at room temperature for 60 min, reacted for 3 min with 0.05% 3,3'-diaminobenzidine (DAB, Sigma) with 0.025% cobalt chloride and 0.02% nickel ammonium sulfate, added for colour intensification, and 0.01% $H_2O_2$ in PBS (pH 7.4). The sections were counterstained with 0.1% aqueous basic fuchsin for 20 min, differentiated with 95% ethanol for 20s, dehydrated with 100% ethanol, cleared in xylene and coverslipped with Permount.

### *Enumeration of BUdR-labelled nuclei*

The labelling index (LI), the ratio of labelled to total nuclei, is adopted as the principal parameter for the present analysis. The use of this ratio obviates the need to use correction methods to compensate for nuclei split by the microtome knife (Unterwood, 1970). Nuclei of endothelial cells, typically distinctive for their elongated configuration and/or proximity to a capillary lumen, were excluded from the enumerations (Fig. 2C,F).

The analysis was conducted in a sector measuring 100 μm in length in the coronal plane within the dorsomedial cerebral wall (Fig. 2A,B; Gadisseux *et al.*, 1989). By means of a suitably calibrated ocular reticule, this sector was subdivided into strata (bins) parallel to the ventricular surface and 10 μm in height (Fig. 2G). These bins were numbered I, II, III and so on from the ventricular surface outward. During the 3.0 h period of the present analysis (9:30 am–12:30 pm), this sector of the cerebral wall increased in thickness from approximately 100 to 120 μm, an increase due entirely to expansion of the primordial plexiform zone (PPZ, Marin-Padilla, 1971, 1978). The VZ remained unchanged in thickness.

For each section, using a × 100 oil immersion objective, labelled and unlabelled nuclei were scored with respect to their bin location. Nuclei on the boundary between two bins were assigned to the bin closer to the ventricle. It was decided arbitrarily to include those touching the medial rather than the lateral margin.

### *The 'LI profile' for each time–dose experiment*

For each time–dose experiment, LI was determined as an average value for each of the bins. These averages were derived as follows. For each brain the LI was determined for each of the bins in four non-adjacent sections included within a series of ten consecutive sections. (In practice, this was every other section in a series of seven consecutive sections except where sections in the series were marred in some way that made them unsuitable.) First the numbers of BUdR-positive and BUdR-negative nuclei in each bin in each of the four sections in a single brain were separately summed. The fraction of BUdR-positive nuclei with respect to the total number of nuclei for each bin provided the average LI for the four sections taken from the single brain. An average LI was then calculated for each bin across the entire series of six brains obtained from the fetuses in two litters and plotted as a function of bin location ('LI profile', Fig. 2G). The standard error (SE) as a proportion of the mean LI for each of the bins I–VIII, bins of principal interest here, varied from 5 to 10%. This percentage was greater for bins superficial to bin VIII where the LIs were much smaller.

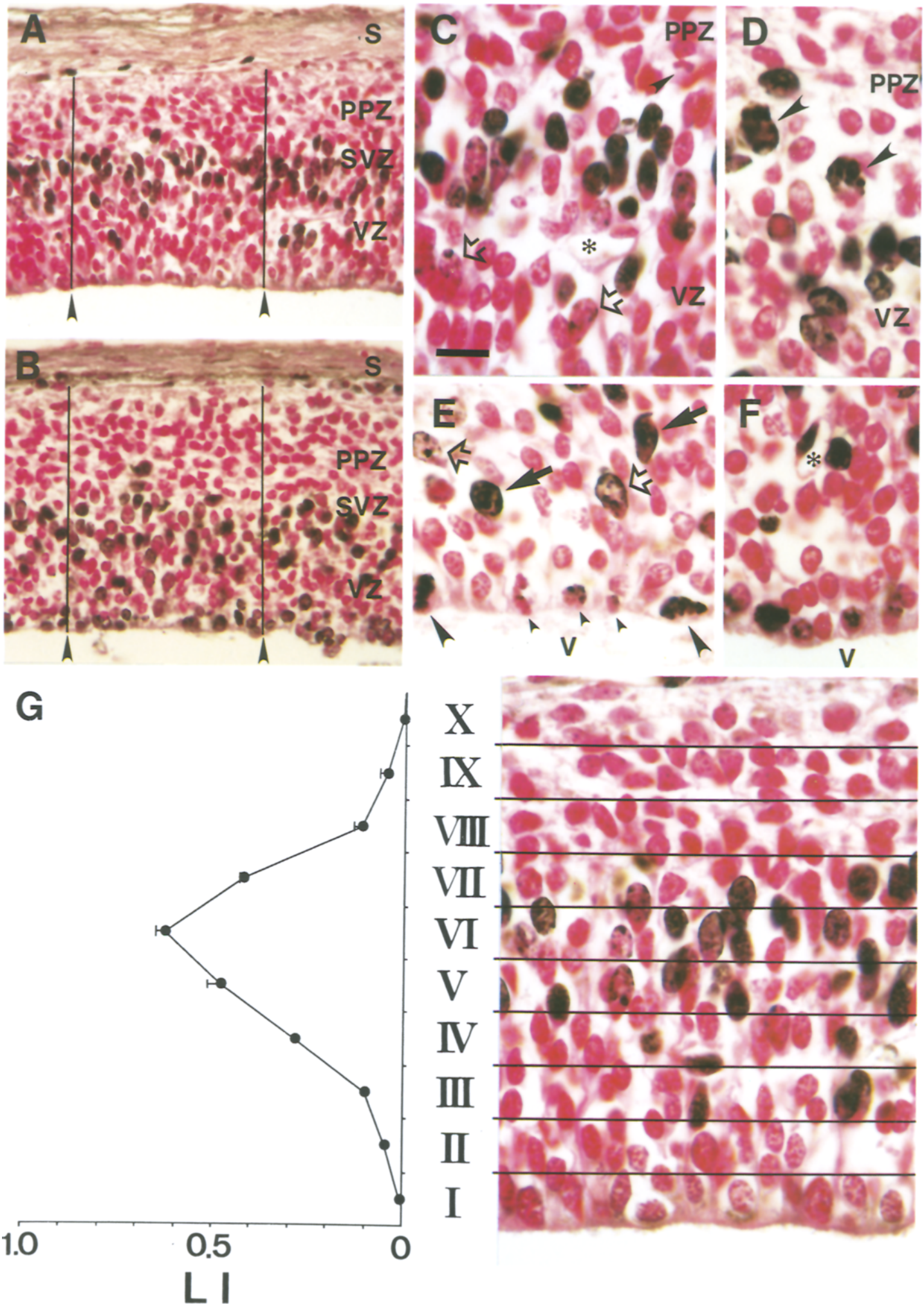
A
S
PPZ
SVZ
VZ
B
S
PPZ
SVZ
VZ
C
PPZ
VZ
D
PPZ
VZ
E
V
F
V
G
1.0
0.5
0
L I
X
IX
VIII
VII
VI
V
IV
III
II
I

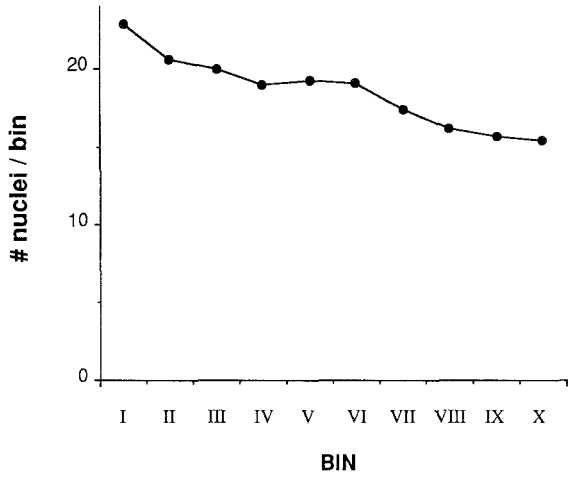


**Fig. 3.** The average number of nuclei per bin within the dorsomedial sector of the E14 cerebral wall. The nuclear density declines gradually across the thickness of the wall. The average number of nuclei is about 23 per bin in bin I and about 19 per bin in bin VI. The SE is less than 3% of the mean of the average number of nuclei.

The number of nuclei counted for the full set of animals was approximately 48 000. There are approximately 20 nuclei per bin in bins I–VI, corresponding to the major part of the VZ. Even within the VZ there is a gradual decline in nuclear density, from about 23 nuclei or mitotic figures per bin near the ventricular surface (bin I) to about 19 nuclei per bin in the outer VZ (bin VI; Fig. 3).

## Results

### THE CEREBRAL WALL AT E14

The analysis was conducted in a dorsomedial sector of the cerebral wall (Fig. 2A,B; Gadisseux *et al.*, 1989), which lies above the lateral ventricle and corresponds approximately to the location of the future primary somatosensory cortex (SI). All animals were killed in the interval 9:10 am–12:30 pm on E14 (Table 1). At this developmental stage, the dorsal sector of the murine cerebral wall is bilaminate, formed of the periventricular generative epithelium and the overlying PPZ (Fig. 2A,B). The generative epithelium is composed principally of the pseudostratified VZ, distinctive for its concentration of mitotic figures at the ventricular surface (His, 1904; Sauer, 1935; Fujita, 1960). Already at E14 a few mitotic figures at the interface between VZ and PPZ mark the location of the secondary proliferative SVZ (Fig. 2C,D). The PPZ contains postmitotic cells embedded in a network of axons.

### CHROMATIN STAINING PATTERNS IN THE VENTRICULAR ZONE

#### *Basic fuchsin counterstain*

The basic fuchsin stain highlights with a scarlet tint the chromatin in nuclei of cells of the cerebral wall (Fig. 2). At a section thickness of 4 μm, each nucleus is

**Fig. 2.** The dorsomedial region of the murine cerebral wall at E14 in 4 μm coronal sections. Nuclei in S-phase are stained immunohistochemically with anti-BUdR antibody. The tissue is counterstained with basic fuchsin. (A) BUdR injection (50 μg $g^{-1}$) at 9:00 am with killing at 9:30 am (E14, 0.5 h). The cobalt-nickel intensified DAB reaction product marks the distribution of nuclei which have incorporated BUdR during S-phase whereas BUdR-negative nuclei stained only by basic fuchsin are scarlet. Each nucleus may be unambiguously distinguished from its neighbours and scored as BUdR positive or negative. The cerebral wall is comprised of a proliferative zone (ventricular zone, VZ, and subventricular zone, SVZ) and a primordial plexiform zone (PPZ). (B) Two BUdR injections (50 μg $g^{-1}$) at 9:00 am and 12:00 noon with killing at 12:30 pm. The zone of labelled nuclei has extended inward to the ventricular suface. For (A) and (B), the 100 μm wide sector upon which the quantitative analyses are based is enclosed within the vertical lines indicated by filled arrowheads. S marks the skull in (A) and (B). (C) S-phase zone and adjacent PPZ from (A) at higher magnification. A BUdR negative nucleus in M-phase (filled arrowhead) belongs to the incipient SVZ. Nuclei with partial staining where only clumps of chromatin are stained (pattern 3; see also description in text) are marked with open arrows. The nucleus of an endothelial cell (above and to the right of the asterisk within the capillary lumen) is elongated and readily distinguished from the proliferative neuronal or neuroglial progenitor cells of the VZ and SVZ. (D–F) BUdR injection (50 μg $g^{-1}$) at 9:00 am and 10:30 am with killing at 11:00 am. (D) The chromatin of nuclei in M-phase within the SVZ (filled arrowheads) is labelled. The chromatin in the mitotic figure to the right is partially labelled (pattern 3; see text). (E) At the ventricular surface, 100% of cells in M-phase are labelled, some partially (pattern 3; small arrowheads), and some diffusely (pattern 1; large arrowheads). Diffusely labelled nuclei with densely (pattern 1; filled arrows) or lightly (pattern 2; open arrows) stained chromatin are at an intermediate depth. (F) The BUdR-labelled nucleus of an endothelial cell lines a capillary (above and to the left of the asterisk in the capillary lumen). V = ventricle in (E) and (F). Scale bar in C = 10 μm. Magnification in (D–F) the same as in (C). (G) BUdR injection (50 μg $g^{-1}$) at 9:00 am with killing at 9:30 am. The 100 μm sector for quantitative analysis is partitioned into a series of horizontal bins as illustrated in a representative micrograph at the right. The labelling index profile for bins I–X for the full series of sections for this time point is presented graphically at the left. Each point on this curve is the average LI for a given bin as determined for six separate brains taken from foetuses in two litters. This distribution is taken as the standard for saturation labelling of nuclei in S-phase for Figs. 5A–9A in which the areas under this curve have been shaded. The peak LI lies in bin VI which is within the VZ proper. Although not sharply demarcated by architectonic criteria, the SVZ corresponds approximately to bins VII and VIII while the PPZ corresponds approximately to bins IX and X. The standard errors (bars) for the LI for each bin are between 5% and 10% of the mean LI.

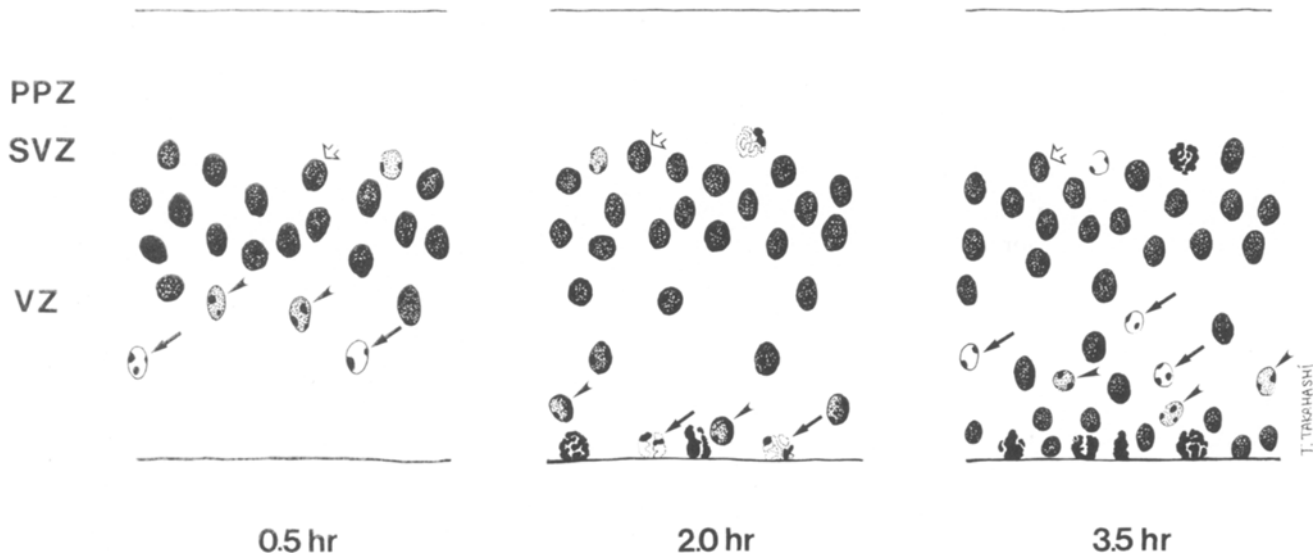


**Fig. 4.** Schematic representation of the distribution of three different staining patterns among BUdR-labelled nuclei when BUdR (50 $\mu g\ g^{-1}$) was injected according to the cumulative labelling schedule, and embryos were killed at 0.5, 2.0 and 3.5 h following the initial injection at 9:00 am on E14. BUdR-positive nuclei and M-phase chromatin are stained according to three patterns: (1) diffuse and dense staining of the entire nucleus or the entire chromatin mass of cells in mitosis (open arrows), (2) diffuse and light staining of all chromatin of interphase cells with discernible staining of clumps of chromatin (arrowheads) and (3) partial staining limited to clumped chromatin within nuclei of interphase cells or only a part of the chromatin mass of cells in mitosis (filled arrows). At 0.5 h nuclei illustrating these patterns are distributed in the order 1-2-3 toward the ventricle. By 2.0 h the chromatin of all mitotic figures is labelled either partially (pattern 3; filled arrows) or diffusely (pattern 1). Pattern 2 nuclei (arrowheads) are distributed at a short distance from the ventricular surface. By 3.5 h all cells in M-phase are pattern 1. Pattern 3 (filled arrows) and pattern 2 (arrowheads) nuclei, both smaller than at 0.5 h, are at an intermediate depth in the VZ.

unambiguously distinguishable from its neighbours throughout the full thickness of the section. Both euchromatin and heterochromatin can be recognized by their differential patterns of distribution (Brown, 1966). The stained euchromatin forms a diffuse investment of the inner aspect of the nuclear envelope thereby providing a sharply defined outline of the nucleus of cells not in M-phase. The stained heterochromatin, by contrast, is distributed in clumps at the inner nuclear membrane as well as throughout the interior of the nucleus of cells in interphase.

*BUdR staining*

The jet-black cobalt-nickel intensified DAB reaction product, marking the distribution of BUdR, provides a dramatic contrast to the scarlet of the cells stained only with basic fuchsin (Fig. 2). Because at any depth in the tissue section the DAB reaction product is in the focal plane of the labelled nucleus, there is no ambiguity in identification of labelled nuclei. There is virtually no background staining so that minimally recognizable staining within a nucleus identifies a cell labelled in S-phase. In both these respects the BUdR method has advantages over $^3$H-TdR autoradiography (see Miller & Nowakowski, 1988). In the autoradiographic method reduced silver grains marking a cell lie in the emulsion layer overlying the tissue. Further, sensitivity of the autoradiographic method is decreased by the fact that there is invariably some background density of grains in the emulsion to be exceeded as a threshold for a nucleus to be considered labelled.

The density and patterns of distribution of DAB reaction product are observed to vary substantially among labelled nuclei in the same histological preparations. There are three distinct patterns of staining (Figs 2,4): (1) diffuse and dense staining of the entire nucleus or the entire chromatin mass of cells in mitosis, (2) diffuse and light staining of the entire nucleus of interphase cells with discernible staining of clumps of chromatin (Fig. 2E), and (3) partial staining limited to clumped chromatin within nuclei of interphase cells (Fig. 2C) or a small part of the chromatin mass of cells in mitosis (Figs. 2D–F). The clumped chromatin and diffusely distributed chromatin stained with BUdR appear to be heterochromatin and euchromatin, respectively. The former is known to be replicated near the end of S-phase (Lima-de-Faria & Jaworska, 1968).

The distribution within the VZ of nuclei representing the different staining patterns changes systematically with survival time following BUdR injection (Fig. 4). These changes in distribution of labelled nuclei with variation in survival time were most completely charted in experiments where the dose of

BUdR was 50 μg g$^{-1}$. The findings with the more limited sets of experiments where the dose was 25 μg g$^{-1}$ or 6.25 μg g$^{-1}$ were comparable. With the smallest dose, the general density of staining was significantly reduced in all labelled nuclei. No attempt was made to determine if there were variations in the proportional representation of the three patterns of chromatin staining under the varied conditions of labelling.

If the survival time was limited to 0.5 h (Fig. 2A,C,G), the majority of labelled nuclei, presumably still in S-phase, were confined to the outer region of the VZ to be referred to as the 'S-phase zone' (vide infra) and were diffusely and densely labelled (i.e., pattern 1). A small number of labelled nuclei with staining pattern 3 were observed to be positioned closer to the ventricular surface (Fig. 2C). Because of their location and the fact that only heterochromatin (and not euchromatin) appears to have stained in these nuclei, they are assumed to have moved from S-phase to G2-phase during the 30 min survival time.

If the survival time was extended to 2.0 h, all mitotic figures were labelled, the majority according to pattern 1 but some according to pattern 3 (Fig. 2E,F). A few nuclei stained with pattern 2 were found at an intermediate depth between the S-phase zone and the ventricular surface (Fig. 2E). With the survival time extended to 3.5 h, a small number of nuclei stained according to pattern 3 were again seen at an intermediate depth (Fig. 4). These were smaller than those observed at 0.5 h and are probably the nuclei of cells which have completed mitosis and entered G1-phase.

All three of these staining patterns were also encountered in the SVZ. There were no obvious shifts in their distribution with variation in survival times (Figs 2D,4).

## DEFINITION OF 'SATURATION' LABELLING OF S-PHASE NUCLEI

The distribution of cells in S-phase and those that have left S-phase over the 30 min following the single injection at 9:00 am is shown in Fig. 2G. (For reference, the area under this curve is shown as a shaded area in Figs 5A–9A). The maximum LI for this curve is approximately 0.6 and lies in bin VI. The LI profiles obtained with cumulative doses of BUdR (max = 50 μg g$^{-1}$) through 3.5 h are illustrated in Fig. 5. With repeated injections over the experimental time interval of only 3.5 h, the configuration of the LI profile changes only in bins I–III. This change presumably occurs as labelled nuclei move inward toward bin I (i.e., the ventricular surface) and enter M-phase. There is only a minimal rise in LIs in the abventricular shoulder of the curve, reflecting, presumably, a relatively small amount of proliferative activity in the SVZ. The differentials in bin LIs with time (difference between LIs at any two time points) in the cumulative labelling experiments are plotted in Fig. 5B.

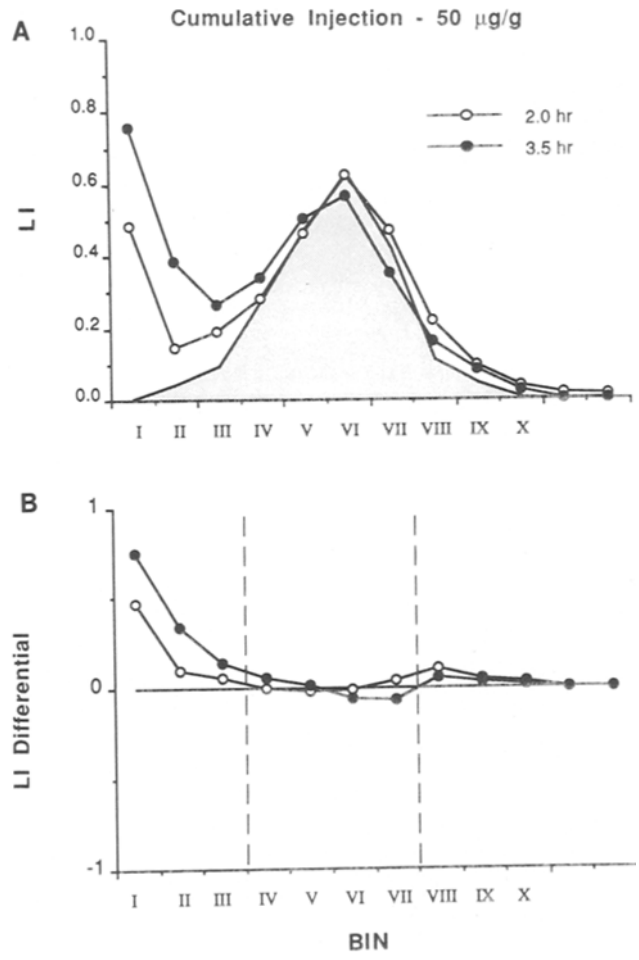


**Fig. 5.** (A) Graphic representation of cumulative LI profiles at 2.0 and 3.5 h following an initial injection of BUdR (50 μg g$^{-1}$) at 9:00 am in comparison to the standard LI profile at 0.5 h after injection from Fig. 2G (shaded area). Each point on the curves is the average LI for a given bin as determined for six separate brains taken from foetuses in two litters. SEs for each bin are between 5–10% of the mean LI. (B) Graphic representation of the LI differentials for the 2.0 and 3.5 h time points with respect to the 0.5 h, or standard, LI profile. There is virtually no change in LI profiles through 3.5 h in bins IV–VII, corresponding to the 'S-phase zone' (enclosed by broken vertical lines in Figs 5B–9B).

Because the LI profile in bins IV–VII remains constant (i.e., the differentials equal zero) throughout the 3.5 h interval of cumulative labelling, we designate this zone of the VZ as the S-phase zone (enclosed within broken vertical lines in Figs 5B–9B). Also, since the area under the LI profile in this zone (summated LIs for bins IV–VII) does not change under these conditions of cumulative labelling, we assume that the entire population of cells in S-phase has been labelled. We refer to this complete labelling of the S-phase population as saturation labelling. The 3.5 h interval

used here is too brief to allow labelled postmitotic cells to re-enter S-phase. This assumption has been confirmed by subsequent experiments which establish that the LI in the S-phase zone reaches 1.0 if cumulative labelling is continued for an interval longer than the length of the cell cycle minus the length of S-phase (Takahashi *et al.*, 1990; cf Waechter & Jaensch, 1972).

### VARIED CONDITIONS OF LABELLING

It is to be expected that saturation labelling of S-phase nuclei will be achieved only when they are exposed to some concentration of BUdR which is at or above a threshold for access to intracellular pathways of incorporation into DNA. It is assumed that an effective labelling concentration will be achieved only after a finite interval following administration of the label. It will be sustained for only a finite interval before the label begins to be cleared from the tissue. The period of time during which tissue concentration of BUdR is sufficient to label nuclei in S-phase as well as the proportion of S-phase nuclei that are labelled may be expected to vary with the magnitude of the dose employed. The following experiments probe these relationships between variation in the dose of BUdR and the duration and effectiveness of labelling.

#### *Long survival times and saturation labelling*

The LI profiles in the S-phase zone (bins IV–VII) are indistinguishable at 0.5 h and 2.0 h after a single injection of BUdR at 50 $\mu g\ g^{-1}$ (Fig. 6). This means that the maximum dose employed in these experiments (50 $\mu g\ g^{-1}$), delivered in a single injection, results in

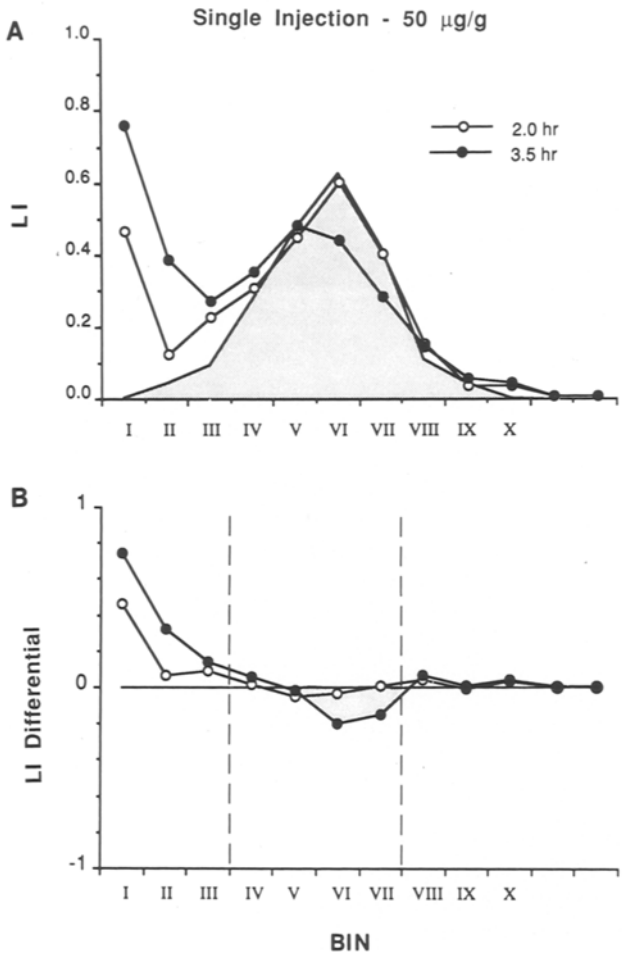


**Fig. 6.** (A) Graphic representation of LI profiles at 2.0 and 3.5 h following a single dose of BUdR (50 $\mu g\ g^{-1}$) at 9:00 am in comparison to the standard LI profile (0.5 h after injection; shaded area). SEs for each bin are between 5–10% of the mean LI. (B) Graphic representation of the LI differentials for the 2.0 and 3.5 h time points with respect to the standard LI profile. Subsaturation (shaded area) occurs on the abventricular side of the S-phase zone (broken lines) at 3.5 h but not at 2.0 h.

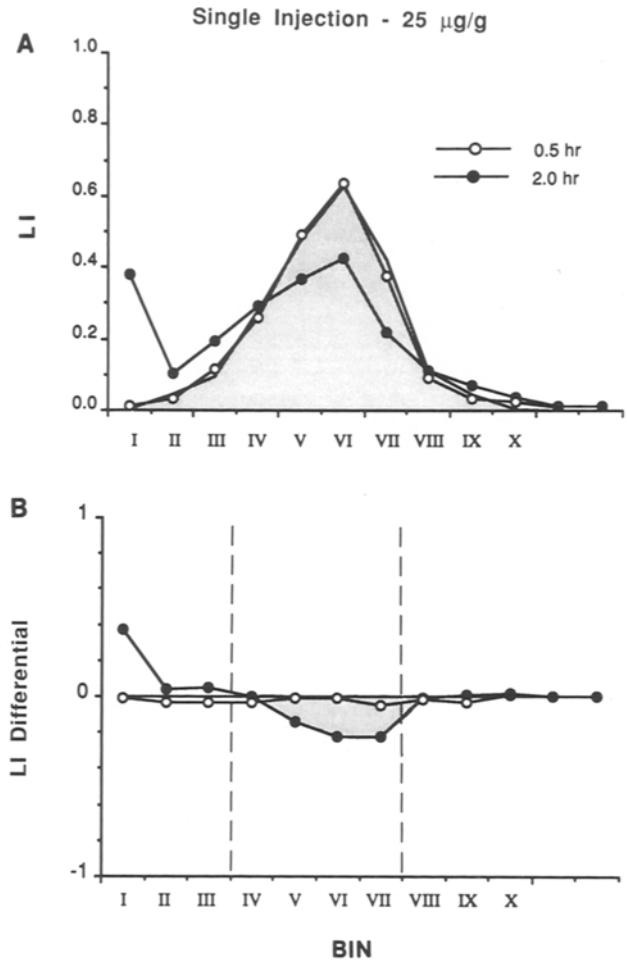


**Fig. 7.** (A) Graphic representation of LI profiles at 0.5 and 2.0 h following a single dose of BUdR (25 $\mu g\ g^{-1}$) at 9:00 am in comparison to the standard LI profile (0.5 h after 50 $\mu g\ g^{-1}$ injection; shaded area). SEs for each bin are between 5–10% of the mean LI. (B) Graphic representation of the LI differentials for the 0.5 and 2.0 h time points with respect to the standard LI profile. Subsaturation (shaded area) occurs on the abventricular side of the S-phase zone (broken lines) at 2.0 h but not at 0.5 h.

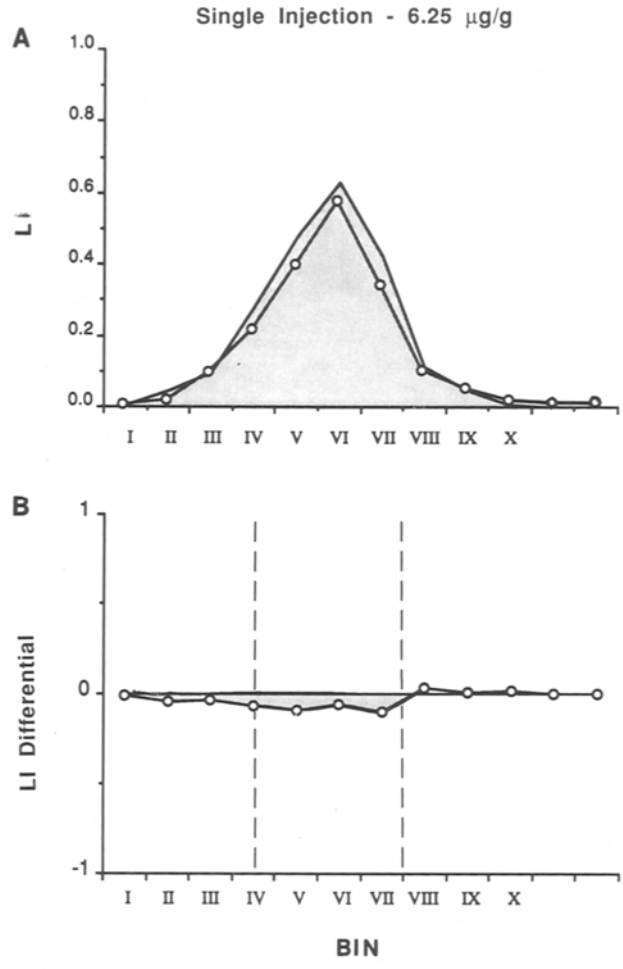


**Fig. 8.** (A) Graphic representation of LI profile at 0.5 h following a single dose of BUdR (6.25 $\mu g\ g^{-1}$) at 9:00 am in comparison to the standard LI profile (0.5 h after 50 $\mu g\ g^{-1}$ injection; shaded area). SEs for each bin are between 5–10% of the mean LI. (B) Graphic representation of the LI differentials between the two profiles. Subsaturation (shaded area) is observed throughout the S-phase zone (broken lines).

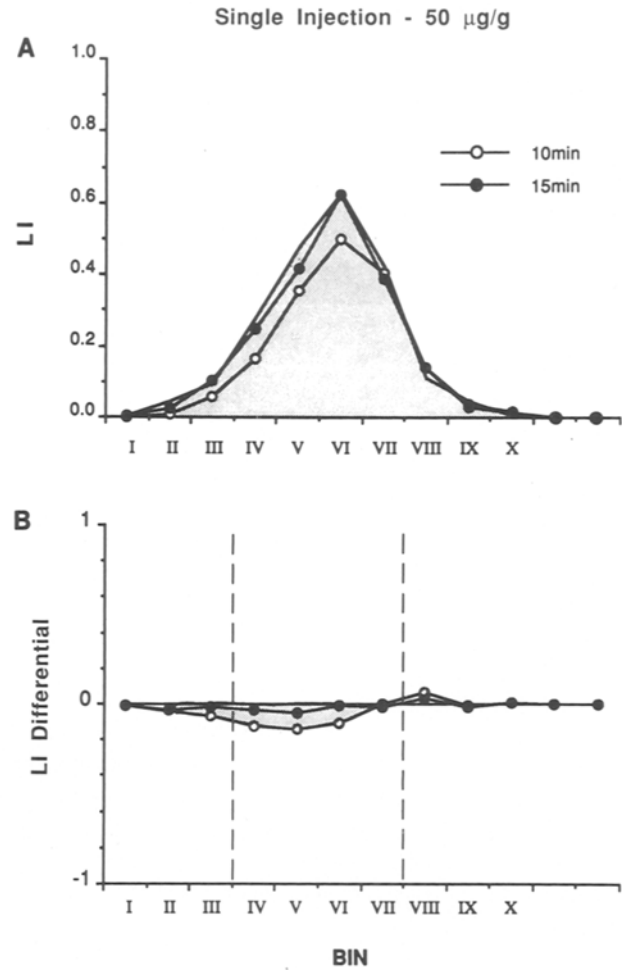


**Fig. 9.** (A) Graphic representation of LI profiles at 10 and 15 min following a single dose of BUdR (50 $\mu g\ g^{-1}$) at 9:00 am in comparison to the standard LI profile (0.5 h after 50 $\mu g\ g^{-1}$ injection; shaded area). SEs for each bin are between 5–10% of the mean LI. (B) Graphic representation of the LI differentials for the 10 and 15 min time points with respect to the standard LI profile. Subsaturation (shaded area) occurs on the ventricular side of the S-phase zone (broken lines) at 10 but not at 15 min.

saturation labelling of S-phase nuclei which is sustained at the 2.0 h time point. In contrast, by 3.5 h following the maximum dose there is subsaturation labelling in bins VI–VII of the S-phase zone (Fig. 6). The degree of subsaturation, corresponding to the reduction in the area under the curve for bins IV–VII (the S-phase zone), is 17% (Table 2). Thus, the duration of saturation labelling of the S-phase nuclei after a single dose at 50 $\mu g\ g^{-1}$ lies between 2.0 and 3.5 h. By comparison, subsaturation at 2.0 h after a single dose of 25 $\mu g\ g^{-1}$ is 31% (Fig. 7; Table 2). A single dose of 6.25 $\mu g\ g^{-1}$, by contast, was insufficient to obtain saturation labelling of the S-phase nuclei (subsaturation = 17%) even at 30 min following a single injection (Fig. 8; Table 2).

The LI profile in the S-phase zone using either 50 $\mu g\ g^{-1}$ at 3.5 h or 25 $\mu g\ g^{-1}$ at 2.0 h differs from that under saturation labelling conditions in its abventricular but not its ventricular side (Figs 6B,7B). The LI profile of subsaturation labelling at 0.5 h following a single dose of 6.25 $\mu g\ g^{-1}$ is, by contrast, uniformly distributed through the S-phase zone (bins IV–VII; Fig. 8B). The implications of these different patterns of subsaturation labelling in the S-phase zone will be considered in the Discussion.

*Brief survival times and saturation labelling*

If the survival time following a single maximum dose (50 $\mu g\ g^{-1}$) is reduced to 15 min, the LI profile in the S-phase zone (bins IV–VII) is still saturated but becomes subsaturated by 21% if the interval is further reduced to 10 min (Fig. 9, Table 2). Here in contrast to the abventricular distribution of subsaturation

**Table 2.** S-phase saturation level with variable doses and survival

| *Dose* | *Labelling Schedule* | *Survival* | *LI for S-phase zone (Mean + SE)* | | *% Saturation* |
|---|---|---|---|---|---|
| 50 $\mu g\ g^{-1}$ | Cumulative | 2.0 h | 1.83 + .11 | NS | 101.1 |
| | | 3.5 h | 1.77 + .02 | NS | 97.4 |
| | Single | 10 min | 1.43 + .06 | ** | 78.9 |
| | | 15 min | 1.70 + .07 | NS | 93.9 |
| | | 0.5 h | 1.81 + .06 | | |
| | | 2.0 h | 1.74 + .07 | NS | 95.7 |
| | | 3.5 h | 1.51 + .10 | * | 83.5 |
| 25 $\mu g\ g^{-1}$ | Single | 0.5 h | 1.72 + .17 | NS | 94.7 |
| | | 2.0 h | 1.25 + .10 | ** | 69.1 |
| 6.25 $\mu g\ g^{-1}$ | Single | 0.5 h | 1.51 + .09 | * | 83.3 |

LI for S-phase zone = area under the LI profile in the S-phase zone. This is equivalent to the summated LIs for bins IV–VII, averaged for 6 brains.
% saturation = a percentage of 1.81, taken as 100%, which is the area under the 0.5 h, or standard, LI profile for the S-phase zone with saturation labelling.
NS not significant, $p > 0.05$
*$p < 0.05$
**$p < 0.01$

associated with long survival times, the shortest survival time was associated with subsaturation in the ventricular side of the LI profile in the S-phase zone (bins IV–VI; Fig. 9B). Again the implications of this pattern of subsaturation will be considered in the Discussion.

## Discussion

The distribution of S-phase nuclei (LI profile of the S-phase zone) is established here to be quantitatively and positionally stable with the SE value less than 10% of the average for up to 3.5 h under the conditions of cumulative labelling. Because of the stability and reproducibility of the LI profile of the S-phase zone, this method allows quantitative estimates of the degree and zone of subsaturation under other labelling conditions.

The histological method described in the present analysis provides clear resolution of all nuclei of the murine dorsomedial cerebral wall at E14. It allows confident distinction between nuclei which have been labelled by exposure to BUdR during S-phase and those which have not been so labelled. The subdivision of the cerebral wall into bins and the determination of labelling indices for each bin provide a method by which to follow the movement of BUdR-labelled nuclei through the successive steps in the cytokinetic cycle.

The method appears to have strong quantitative reproducibility, as reflected by an SE which is less than 10% of average values for LIs within bins. This feature, in principle, should allow the method to support a broad set of analyses directed toward a quantitative model of neocortical histogenesis. Only the following elementary applications are undertaken at this initial stage of study.

### DIFFERENTIAL PATTERNS OF NUCLEAR STAINING WITH BUdR

Heterochromatin is known to be replicated near the end of S-phase (Fujita, 1965; Brown, 1966; Lima-de-Faria & Jaworska, 1968). Thus, partially labelled nuclei in which only clumps of heterochromatin are stained (pattern 3) have probably been exposed to BUdR only near the end of S-phase. Nuclei with this pattern of labelling were observed when survival time was 0.5 h. They are preferentially located between the S-phase zone and the ventricular surface. Only a few nuclei with this pattern of labelling were present in the SVZ at 0.5 h survival. It seems likely that these cells in the VZ and SVZ represent a subpopulation that has moved out of S-phase to enter G2-phase during the 0.5 h interval following their exposure to BUdR.

When the survival time is extended to 2.0 h, the partially labelled nuclei within the VZ (pattern 3) have shifted further inward toward the ventricular surface. At 3.5 h they have again moved outward, though not as far as the S-phase zone. The nuclei are smaller than those observed at 0.5 h suggesting that they have completed mitosis and have entered G1-phase. Thus, the nuclear population with this distinctive staining pattern probably marks the leading edge of the interkinetic wave within the VZ. Such partially labelled nuclei are also recognized in the SVZ but undergo no recognizable pattern of interkinetic movement.

The diffusely and lightly labelled nuclei (pattern 2) appear systematically to trail the movement of the population of nuclei with pattern 3 labelling. These pattern 2 nuclei are assumed to have been exposed to BUdR through a somewhat longer period of S-phase.

### FUNCTIONAL COMPARTMENTALIZATION OF THE VZ

For several decades it has been believed that the nuclei of the proliferative cells are distributed in different depths of the VZ, depending upon their positions in the cytokinetic cycle (His, 1904; Sauer, 1935; Sauer & Walker, 1959; Sidman *et al.*, 1959; Fujita, 1960, 1963; Hinds & Ruffett, 1971). The present study provides, for the first time, a quantitative profile of distribution of the position of nuclei in S-phase and their movement through G2 into M-phase. With regard to the VZ proliferative population of the early E14 embryos considered here, S-phase is concentrated in bins IV–VII (i.e., in the S-phase zone), M-phase occurs only in bin I (i.e., at the ventricular surface) while cells in G2-phase are probably most concentrated in bins II and III.

The LI profile in the S-phase zone, bins IV–VII, varies depending upon whether the dose of BUdR is sufficient to provide saturation labelling throughout S-phase. Three different patterns of subsaturation were encountered in these studies. These depended upon the dose of a single BUdR injection and the survival time following the single injection. The various positions of the subsaturation, with respect to the LI profile in the S-phase zone were: abventricular, ventricular or uniform throughout the S-phase zone. The abventricular pattern was encountered where the LI profile of the S-phase zone was initially saturated but then became subsaturated (3.5 h after 50 $\mu g\, g^{-1}$ and 2.0 h after 25 $\mu g\, g^{-1}$; Figs 6,7). Under these conditions subsaturation presumably reflects the continued entry of cells into S-phase from G1. These newly entered cells do not become labelled because the concentration of BUdR has fallen below threshold. The position of these unlabelled S-phase nuclei in bins VI–VII indicates that the cells of the pseudostratified VZ epithelium initiate DNA replication with their descending process maximally elongated. The cell nucleus appears to approach the ventricular surface as DNA synthesis continues.

The ventricular pattern of subsaturation was encountered under conditions where the survival time after injection was too brief for saturation labelling to occur (10 min after 50 $\mu g\, g^{-1}$; Fig. 9). The subsaturation pattern occurring at 10 min is limited to bins IV–VI, nuclei on the ventricular side of the S-phase zone and presumably, therefore, nearing the end of S-phase. This observation suggests that BUdR-incorporation is less efficient near the end of S-phase.

The subsaturated LI profile seen in bins IV–VI with the 10 min period of labelling, in contrast to the LI profile with saturated labelling seen with the 15 min period of labelling, probably does not reflect a simple matter of nuclear movement occurring in a five minute interval. This possibility might be viewed as an alternative though unlikely explanation for the ventricular pattern of subsaturation at 10 min. The five minute difference may be assumed to be an insignificant period in terms of the rate of nuclear movement through S-phase.

It is known that nuclei replicate heterochromatin near the end of their DNA synthetic period (Lima-de-Faria & Jaworska, 1968). Because nuclei which are near the end of S-phase appear to be on the ventricular side of the S-phase zone, heterochromatin synthesis is probably occurring in nuclei in this position. That is, nuclei near the end of S-phase and synthesizing heterochromatin may incorporate BUdR with reduced efficiency in comparison to early stages of DNA replication.

If the dose was only 6.25 $\mu g\, g^{-1}$ and the period of survival was 30 min, there was a small portion of unlabelled S-phase nuclei in each bin of the entire S-phase zone (Fig. 8). This suggests that a small but fairly constant population of cells, without bias as to stage of S-phase, did not incorporate sufficient BUdR to reach a staining threshold for detection in the histological sections. Possibly the concentration of BUdR gaining access to endogenous deoxynucleotide pools of the S-phase nuclei was near some critical threshold for detection with this low BUdR dose (de Fazio *et al.*, 1987); this possibility was not further explored in these experiments.

### FUTURE APPLICATIONS

The present analysis establishes guidelines for the design of experiments concerned with the lengths of the successive phases of the cytokinetic cycle as well as a more comprehensive functional compartmentalization of the VZ. Thus, 50 $\mu g\, g^{-1}$ of BUdR will assure saturation labelling of nuclei in S-phase for an interval of 15 min through 2.0 h postinjection. To our knowledge this is the first determination of the effective labelling time for an S-phase marker as applied to generative populations of the mammalian CNS. Previous measurements of this interval have relied on the fact that exogenous DNA precursor may be detected in the blood following an injection (for references, see Nowakowski & Rakic, 1974; deFazio *et al.*, 1987). Clearly, tissue concentrations of a DNA precursor following a single injection may or may not rise and fall in a predictable way with concentrations in the circulating plasma. Furthermore, it appears from these experiments that some range of tissue concentrations of BUdR below a threshold required for saturation labelling will still label a portion of the cells in S-phase. Finally, this analysis establishes that

injections of 50 $\mu g\, g^{-1}$, spaced at intervals no greater than every 2 h, will assure continuous saturation labelling of S-phase nuclei, independent of S-phase length.

Finally, our data provide the first insight into the *systematic* relationship between stage of the cell cycle and the position of the nucleus within the VZ. In particular, our data indicate that when a VZ cell enters S-phase, its nucleus is furthest away from the ventricular surface (i.e., at its maximum abventricular position), that the nucleus of a cell in S-phase moves towards the ventricular surface, and that, as the cell enters G2-phase, its nucleus is about midway across the VZ (i.e., in bins III–IV). Most intriguingly, our data indicate that during the *entire* G1-phase, the nucleus moves outward from the ventricular surface towards the outer portion of the VZ. Further work is necessary to confirm and extend these observations.

## Acknowledgements

Supported by NIH grants NS12005 and NS28061 and NSF grant BNS8921020. Valuable discussions with Pradeep Bhide, Igor Rosenwald and Douglas Frost and their critical comments on earlier versions of the manuscript; technical assistance by Margaretha Jacobson and helpful comments on the manuscript by Nancy Hayes are gratefully acknowledged.

## References

ALTMAN, J. (1966) Proliferation and migration of undifferentiated precursor cells in the rat during postnatal gliogenesis. *Experimental Neurology* **16**, 263–78.

ANGEVINE, J. B. & SIDMAN, R. L. (1961) Autoradiographic study of cell migration during histogenesis of the cerebral cortex in the mouse. *Nature* **192**, 766–8.

ATLAS, M. & BOND, V. P. (1965) The cell generation cycle of the eleven-day mouse embryo. *Journal of Cell Biology* **26**, 19–24.

BERRY, M., ROGERS, A. W., EAYRS, J. T. (1964) Pattern of cell migration during cortical histogenesis. *Nature* **203**, 591–3.

BOULDER COMMITTEE (1970) Embryonic vertebrate nervous system: revised terminology. *Anatomical Record* **166**, 257–62.

BROWN, S. W. (1966) Heterochromatin. *Science* **151**, 417–25.

CAVINESS, V. S., JR. (1982) Neocortical histogenesis in normal and reeler mice: a developmental study based upon [3H]thymidine autoradiography. *Developmental Brain Research* **4**, 293–302.

CAVINESS, V. S., JR., & SIDMAN, R. L. (1973) Time of origin of corresponding cell classes in the cerebral cortex of normal and reeler mutant mice: an autoradiographic analysis. *Journal of Comparative Neurology* **148**, 141–52.

DEFAZIO, A., LEARY, J. A., HEDLEY, D. W., & TATTERSALL, H. N. (1987) Immunohistochemical detection of proliferating cells in vivo. *Journal of Histochemistry and Cytochemistry* **35**, 571–7.

FUJITA, S. (1960) Mitotic pattern and histogenesis of the central nervous system. *Nature* **185**, 702–3.

FUJITA, S. (1963) The matrix cell and cytogenesis in the developing nervous system. *Journal of Comparative Neurology* **120**, 37–42.

FUJITA, S. (1965) Chromosomal organization as a genetic basis of cytodifferentiation in multicellular organisms. *Nature* **206**, 742–4.

FUJITA, S., HORII, M., TANIMURA, T., & NISHIMURA, H. (1964) $H^3$-thymidine autoradiographic studies on cytokinetic response to X-ray irradiation and to thio-TEPA in the neural tube of mouse embryos. *Anatomical Record* **149**, 37–48.

FUJITA, S., SHIMADA, M., & NAKAMURA, T. (1966) $H^3$-thymidine autoradiographic studies on the cell proliferation and differentiation in the external and the internal granular layers of the mouse cerebellum. *Journal of Comparative Neurology* **128**, 191–208.

GADISSEUX, J. -F., EVRARD, P., MISSON, J. -P., & CAVINESS, V. S., JR. (1989) Dynamic structure of the radial glial fiber system of the developing murine cerebral wall. An immunocytochemical analysis. *Developmental Brain Research* **50**, 56–67.

GRATZNER, H. G. (1982) Monoclonal antibody to 5-bromo- and 5-iododeoxyuridine; a new reagent for detection of DNA replication. *Science* **218**, 474–5.

HINDS, J. W., & RUFFETT, T. L. (1971) Cell proliferation in the neural tube: an electron microscopic and Golgi analysis in the mouse cerebral vesicle. *Zeitschrift fur Zellforschung* **115**, 226–64.

HIS, W. (1904) Die Entwicklung des Menschlichen Gehirns wahrend der ersten Monate. Leipzig: von S. Hirzel, pp. 1–176.

KAUFFMAN, S. L. (1966) An autoradiographic study of the generation cycle in the ten-day mouse embryo neural tube. *Experimental Cell Research* **42**, 67–73.

KAUFFMAN, S. L. (1968) Lengthening of the generation cycle during embryonic differentiation of the mouse neural tube. *Experimental Cell Research* **49**, 420–4.

LIMA-DE-FARIA, A., & JAWORSKA, H. (1968) Late DNA synthesis in heterochromatin. *Nature* **217**, 138–42.

MARES, V. & BRUCKNER, G. (1978) Postnatal formation of neural cells in the rat occipital cerebrum: an autoradiographic study of the time and space pattern of cell division. *Journal of Comparative Neurology* **177**, 519–28.

MARIN-PADILLA, M. (1971) Early prenatal ontogenesis of the cerebral cortex (neocortex) of the cat (Felis domestica). A Golgi study. I. The primordial neocortical organization. *Zeitschrift fur Anatomie und Entwicklungsgeschichte* **134**: 117–45.

MARIN-PADILLA, M. (1978) Dual origin of the mammalian neocortex and evolution of the cortical plate. *Anatomy and Embryology* **152**, 109–26.

MILLER, M. W., & NOWAKOWSKI, R. S. (1988) Use of bromodeoxyuridine-immunohistochemistry to examine the proliferation, migration and time of origin of cells in the central nervous system. *Brain Research* **457**, 44–52.

MILLER, M. W., & NOWAKOWSKI, R. S. (1991) Effect of

prenatal exposure to ethanol on the cell cycle kinetics and growth fraction in proliferative zones of the fetal rat cerebral cortex. *Alcoholism and Clinical Experimental Research* **15**, 229–32.

MISSON, J.-P., AUSTIN, C. P., TAKAHASHI, T., CEPKO, C. L. & CAVINESS, V. S., JR. (1991) The alignment of migrating neuronal cells in relation to the murine neopallial radial glial fiber system. *Cerebral Cortex* **1**, 221–9.

NOWAKOWSKI, R. S., & RAKIC, P. (1974) Clearance rate of exogenous 3H-thymidine from the plasma of pregnant rhesus monkey. *Cell and Tissue Kinetics* **7**, 189–94.

NOWAKOWSKI, R. S. & RAKIC, P. (1981) The site of origin and route and rate of migration of neurons to the hippocampal region of the rhesus monkey. *Journal of Comparative Neurology* **196**, 129–54.

NOWAKOWSKI, R. S., LEWIN, S. B. & MILLER, M. W. (1989) Bromodeoxyuridine immunohistochemical determination of the lengths of the cell cycle and the DNA-synthetic phase for an anatomically defined population. *Journal of Neurocytology* **18**, 311–8.

RAKIC, P. (1972) Mode of cell migration to the superficial layers of fetal monkey neocortex. *Journal of Comparative Neurology* **145**, 61–84.

RAKIC, P. (1978) Neuronal migration and contact guidance in the primate telencephalon. *Postgraduate Medical Journal* **54**, 25–40.

RAKIC, P. (1985) Limits of neurogenesis in primates. *Science* **227**, 1054–6.

RAKIC, P. (1988) Specification of cerebral cortical areas. *Science* **241**: 170–6.

SAUER, F. C. (1935) Mitosis in the neural tube. *Journal of Comparative Neurology* **62**, 377–405.

SAUER, M. E. & WALKER, B. E. (1959) Radioautographic study of interkinetic nuclear migration in the neural tube. *Proceedings of the Society for Experimental Biology and Medicine* **101**, 557–60.

SCHMECHEL, D. E. & RAKIC, P. (1979) Arrested proliferation of radial glial cells during midgestation in rhesus monkey. *Nature* **277**, 303–5.

SHIMADA, M. & LANGMAN, J. (1970) Cell proliferation, migration and differentiation in the cerebral cortex of the golden hamster. *Journal of Comparative Neurology* **139**, 227–44.

SHOUKIMAS, G. M. & HINDS, J. W. (1978) The development of the cerebral cortex in the embryonic mouse: an electron microscopic serial section analysis. *Journal of Comparative Neurology* **179**, 795–830.

SIDMAN, R. L. (1970) Autoradiographic methods and principles for study of the nervous system with thymidine-H3. In NAUTA, W. J. H. & EBBESSON, S. O. E. (eds): *Contemporary Research Methods in Neuroanatomy* New York: Springer, pp. 252–74.

SIDMAN, R. L., MIALE, I. L. & FEDER, N. (1959) Cell proliferation and migration in the primitive ependymal zone: an autoradiographic study of histogenesis in the nervous system. *Experimental Neurology* **1**, 322–33.

SMART, I. (1961) The subependymal layer of the mouse brain and its cell production as shown by autoradiography after thymidine-H3 injection. *Journal of Comparative Neurology* **116**, 325–47.

SMART, I. & LEBLOND, C. P. (1961) Evidence for division and transformation of neuroglia cells in the mouse brain, as derived from radioautography after injection of thymidine-H3. *Journal of Comparative Neurology* **116**, 349–67.

TAKAHASHI, T., JACOBSON, M., NOWAKOWSKI, R. S. & CAVINESS, V. S., JR (1990) Cell cycle kinetics of the E14 murine cerebral ventricular zone: estimates based upon S-phase labelling with BUdR. *Society for Neuroscience Abstracts* **16**, 1147.

TAKAMIYA, T., KOHSAKA, S., TOYA, S., OTANI, M. & TSUKADA, Y. (1988) Immunohistochemical studies on the proliferation of reactive astrocytes and the expression of cytoskeletal proteins following brain injury in rats. *Developmental Brain Research* **38**, 201–10.

UNTERWOOD, E. E. (1970) *Quantitative Stereology*. Reading, MA.: Addison-Wesley.

WAECHTER, R. V. & JAENSCH, B. (1972) Generation times of the matrix cells during embryonic brain development: an autoradiographic study in rats. *Brain Research* **46**, 235–50.